

# PERMITTIVITY AND PERMEABILITY MEASUREMENT METHODS FOR PARTICLE ACCELERATOR RELATED MATERIALS

Christine Vollinger, Fritz Caspers, Erk Jensen, CERN, Geneva, Switzerland

## Abstract

For the special requirements related to particle accelerators, knowledge of the different material parameters of dielectrics and other materials are needed in order to carry out simulations during the design process of accelerator components. This includes also properties of magnetically biased ferrites of which usually little information is available about material characteristics, especially in magnetic bias fields. Several methods of measurement are discussed and compared of which some require delicate sample preparation whereas others can work with unmodified material shapes that makes those methods also suited for acceptance checks on incoming materials delivered by industry. Applications include characterization of different materials, as absorbers in which dielectric losses play an increasing role, as well as low frequency measurements on ferrites that are used for tunable cavities. We present results obtained from both broadband and resonant measurements on different materials determined in the same sample holder. Where possible, the results were confirmed with alternative methods.

## INTRODUCTION

A large variety of particle accelerator materials exist and for most of these the em-material parameters are well known over large frequency ranges. Here we restrict ourselves to *ferrite* materials that serve different purposes in particle accelerators e.g. as em-absorbers to dampen unwanted modes or garnets for RF-cavity tuning. Of these materials broadband electromagnetic data are usually not readily available. Since material losses are of major interest in applications, we measured complex permeability and complex permittivity so that losses can be quantified from  $\tan\delta_m = \frac{\mu''}{\mu'}$  and  $\tan\delta_e = \frac{\epsilon''}{\epsilon'}$ . A precise material knowledge is also required to model these materials in simulation codes.

## MEASUREMENT METHODS

### Coaxial Line Measurement



Figure 1: Picture of coaxial sample holder used for reflection and transmission measurements.

In the coaxial line measurement, a toroidal shaped sample is required to be put into the cross-section making this a destructive testing unsuited e.g. for acceptance checks or

for other quality assurance purposes. We measured with a coaxial line with shorted end, in transmission and for resonant measurements using an FNB type Dezifix from Rohde & Schwarz (see Fig. 1). This method is described in detail in [1], including analyses of measurement error and uncertainty. For reflection permeability measurements, the permittivity has to be known beforehand since only  $s_{11}$  is measured. The material under test is placed directly before the shorted end. Hence,  $s_{11}$  at the measurement port is obtained by transforming the shorted end stepwise along the line which yields the desired transcendent equation for  $\mu_r$ :

$$\sqrt{\mu_r} \tanh\left(\frac{\omega \sqrt{\epsilon_r}}{c_0} l_1 \sqrt{\mu_r}\right) = \frac{2 \sqrt{\epsilon_r}}{1 - s_{11} e^{2\gamma_0(l_{SH} - l_1)}}. \quad (1)$$

Here,  $l_1$  is the sample thickness,  $l_{SH}$  and  $\gamma_0$  denote length and propagation constant of the unloaded part of the sample holder. We used the shorted coaxial line for determining the complex  $\mu_r$  of ferrite samples (garnets and spinells) and also on tuning ferrites (garnets only) where we placed the entire sample holder into a magnetic bias field perpendicular to the RF-magnetic field while frequency sweeps were carried out. This allowed to cross-check data taken with a larger sample holder or other methods (see [2] for details). The complex  $\epsilon_r$  was determined from resonant and non-resonant transmission measurements of which the theory applied to our specific sample holder is given in the next section.

Resonant measurements in the coaxial line are carried out with a thin toroidal sample positioned in the center of the sample holder based on the perturbation theory [3]. In our case, we connected the sample holder on both sides via small adjustable capacitors in the femto-Farad range. The disadvantage of the method is that it only gives values for the resonant frequencies of the set-up. The toroid is placed in the center of the sample holder, i.e. positioned alternately at the maximum electric and magnetic field. Evaluation of the resonant peaks of the unloaded and the loaded structure yields the resonant frequencies  $f_{res,empty,i}$  and  $f_{res,mat,i}$  of the  $i$ -th resonance. From these values, the material data can be determined from:

$$\mu_r = 1 + \frac{(l_{SH} + l_1)}{l_1} \frac{f_{res,empty,i} - f_{res,mat,i}}{f_{res,empty,i}}, \quad (2)$$

where again,  $l_{SH} + l_1$  is the total length of the sample holder,  $l_{SH}$  the length the unloaded part, and  $l_1$  the sample thickness. Results are shown in the next section.

### Transmission Measurement

A sample holder that is tailor-made to the sample size was developed for the transmission measurement. It consists of a center conductor around which the material samples

(tile-shaped) are clamped and is suited for all planar sample sizes. This way, the dimensions of the center conductor are defined by the sample size (see [4] for details), and allow a non-destructive measurement of s-parameters with a vector network analyzer (VNA). This sample holder is currently used for measurements of all types of ferrites, including low-loss materials so that a design is required with open boundaries ideally all around the samples to avoid HOM resonances resulting from the housing. Hence, side walls were either omitted or made of acrylic glass as to be transparent. The ground planes were made of brass. Due to the lack of elasticity of the ferrites, some delicate material handling is required while clamping the tiles around the center conductor. Note that radial air gaps can be cor-

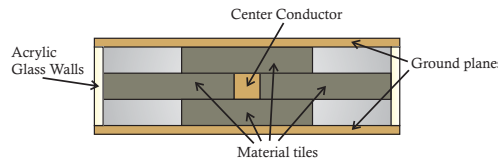


Figure 2: Schematic of the sample holder's cross-section.

rected with formulae found in literature, e.g. [1] whereas the unavoidable azimuthal air gaps can be controlled. From the complex s-parameters,  $\mu_r$  and  $\epsilon_r$  are obtained in one frequency sweep. Our evaluation follows in principle the method shown by Barry [5], however, we had to allow for an impedance of the empty test cell unmatched to that of the VNA system. If  $R$  is the reflection factor at the plane boundaries between the  $50 \Omega$  line and the loaded sample holder, a change in characteristic impedance of the set-up is seen in the propagation constant  $k_1$  in the material and in the complex reflection coefficient  $R$  which reads:

$$R = \left( \frac{Z_1}{Z_0} \sqrt{\frac{\mu_0}{\epsilon_0}} - 1 \right) / \left( \frac{Z_1}{Z_0} \sqrt{\frac{\mu_0}{\epsilon_0}} + 1 \right), \quad (3)$$

where  $Z_0$  denotes the characteristic impedance of the connecting cables and the VNA system, and  $Z_1$  is the input impedance of the unloaded test cell which can be calculated with textbook formulae. The input impedance has to be multiplied by  $\sqrt{\mu_r/\epsilon_r}$  when the sample holder is loaded with material and the propagation constant then reads  $k_1 = k_0 \sqrt{\mu_r \epsilon_r}$ . By evaluating Eqs. (3) with  $k_1$ , the material parameters yield

$$\epsilon_r = \frac{Z_1}{Z_0} \frac{k_1}{k_0} \frac{1-R}{1+R}, \quad \text{and} \quad \mu_r = \frac{Z_0}{Z_1} \frac{k_1}{k_0} \frac{1+R}{1-R}. \quad (4)$$

This way, unmodified material tiles can be used and machining of the ferrite can be avoided.

## MEASUREMENT RESULTS

### Reflection Measurements

Reflection measurements were carried out with a shorted coaxial line to obtain material data for certain frequency ranges as input for simulation programs. Fig. 3 shows the absorber material 4E2 from Ferroxcube for frequency ranges of 10 MHz to 1 GHz and 2 GHz. The frequency range for  $\epsilon_r$

was enlarged due to its dispersive behaviour. Compared to the data given by the supplier, we observe that our samples show the maximum  $\mu'$  at a lower frequency (about 80 MHz) and also that we measure a higher  $\mu'$ . Fig. 4 shows results

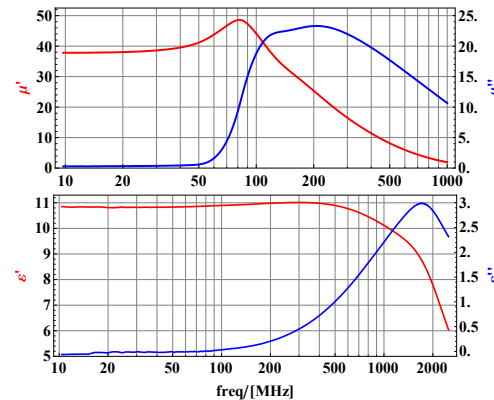


Figure 3: Measurements on absorber material 4E2 from Ferroxcube for different frequency ranges.

for a low-loss garnet (G-510 from Trans-Tech Inc.) which is e.g. used for cavity tuning and carried out in a static magnetic bias field perpendicular to the magnetic RF-field. The set-up for a shorted coaxial line is presented by Eberhardt [2]. The plots show  $\mu_r$ -measurements taken at 1-100 MHz for 3 different values of magnetic bias (solid lines) and compared to the measurements taken with large ferrite rings of the same material (dashed lines). As expected, a difference in absolute values exists due to the fact that the large ferrite rings experience a different magnetic flux distribution within the material when exposed to magnetic fields of the same biasing current (here: biasing currents of 240 A, 80 A and 0 A). Further details can be found in [2].

### Transmission Measurements

The transmission measurement method with its tailor-made sample holder was first used for the measurement of the absorber TT2-111R from Trans-Tech Inc. available in quadratic tiles of a side length  $l=6$  cm and 5 mm thickness. Fig. 5 shows the complex  $\mu$  from the tiles' measurements (solid line, (red)) compared to coaxial line measurements

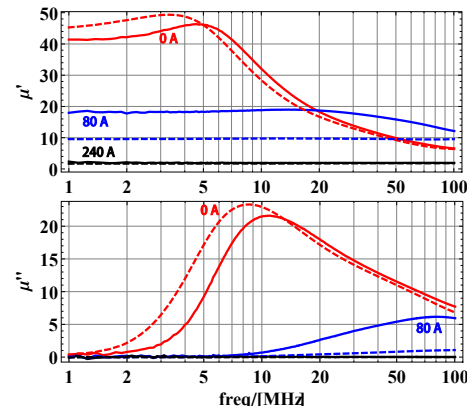


Figure 4: Measurements taken on G-510 in magnetic bias fields, showing the influence of different sample sizes.

taken by the supplier (dashed line, (blue)) and with our coaxial line set-up (dotted line, (black)). For completeness, Fig. 6 gives the measured real part of the relative permittivity showing a decrease of  $\epsilon'$  with increasing frequency. Note that the supplier's specification is  $\epsilon'=12.5 \pm 10\%$ . After the good agreement of the measurements with the supplier's data, we used the method on different absorbers of various sample sizes as ingoing material tests. These measurements of the

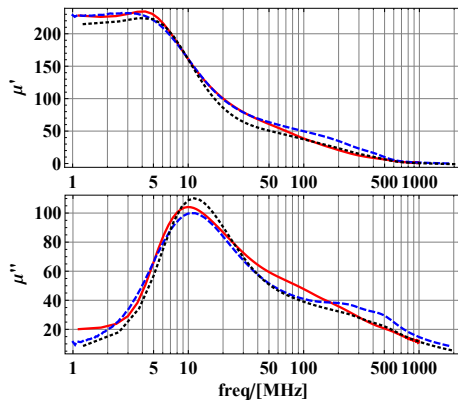


Figure 5: Permeabilities obtained from shorted coaxial line measurements from supplier (dashed (blue)), own set-up (dotted (black)) and data taken on tiles (solid (red)).

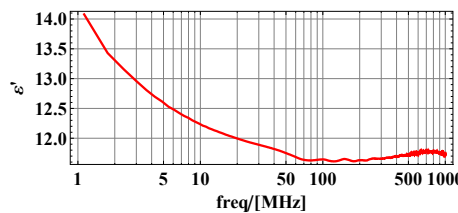


Figure 6: Real part of measured permittivity vs. frequency obtained from measurement taken on tiles.

TT2-111R absorber served as verification of the method and of the sample holder design and show a very good agreement for a frequency range of 1 MHz to 1.3 GHz, except for the range 50-500 MHz where we observe a difference for both  $\mu'$  and  $\mu''$  which, as we will see later is within the material spread (samples from different batches). Further,

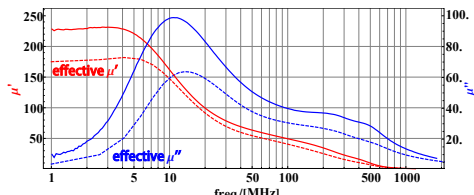


Figure 7: Influence of air gap on permeability due to chamfering (solid), compared with un-chamfered samples (dashed).

we measured the em-properties of absorber samples that underwent an extended heat-treatment [6] at CERN consisting of heating the samples for several hours to 1000 deg C in vacuum before installing them in the accelerators. It was therefore not an option to cut the samples into any sample holder's shape. These samples are chamfered at all corners introducing a notable air gap when they are clamped around

the center conductor. Results from chamfered samples show that chamfers make  $\mu_r$  appear lower than it is (see Fig. 7).

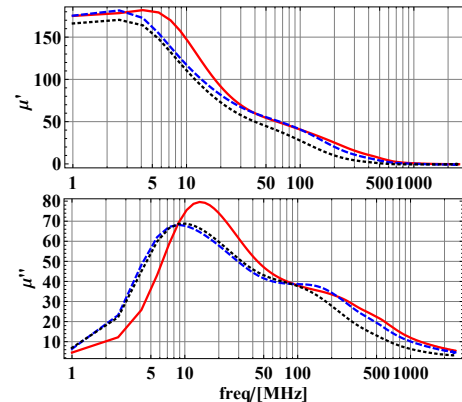


Figure 8: Permeability measured on two different samples after heat treatment ((dashed, blue) and (dotted, black) graphs) compared to new (reference) data (solid, red).

We therefore restricted ourselves to relative measurements taken on fully-chamfered samples to allow the comparison of em-properties of samples before and after heat-treatment (see Fig. 8). It can be seen from the graphs that the heat-treated samples reach their maxima of  $\mu$  at lower frequencies than the untreated ones and that  $\mu''$  generally gets smaller. Note that in the range of 50-500 MHz, the two heat treated samples from the same material batch show a considerable deviation similar to what we already observed in samples from different batches. We consider this effect to be due to material spread.

### Resonant Measurement

The resonant measurement was used as a cross-check of broadband data and gave a good agreement. It was equally used in cases of very low electric losses where the broadband methods are not giving sufficient precision. The specific advantage of the resonant method is that it allows to clearly separate the electric and the magnetic losses by placing the sample in the electric and magnetic field maxima. Results are included in Fig. 3.

### CONCLUSIONS

We present a measurement method for em-parameters of ferrite tiles that avoids machining of the samples and thus is suited e.g. for acceptance tests or for other quality assurance purposes. The measurements were compared to 1-port measurements, as well as transmission and resonant perturbation methods and show a very good agreement.

### REFERENCES

- [1] Baker-Jarvis, J., NIST-publication, no. 1355, 1990.
- [2] Eberhardt, J. et. al., these proceedings.
- [3] Waldron, R. A., IEE, Monogr. 373 E, 1960.
- [4] Vollinger, C. et al., publication in process.
- [5] Barry, W., IEEE Trans. MTT-34, 1986.
- [6] Aberle, O., CERN internal publication.